The Correlation Between Crystal Structure and Nucleation Efficiency of a Lithium (I) Complex on Isotactic Polypropylene

Yaoqi Shi, Zhong Xin

Department of Product Engineering, State Key Laboratory of Chemical Engineering, College of Chemical Engineering, East China University of Science and Technology, Shanghai 200237, China

Received 29 August 2011; accepted 7 October 2011
DOI 10.1002/app.36236
Published online 1 February 2012 in Wiley Online Library (wileyonlinelibrary.com).

ABSTRACT: In this work, 2,2′-methylene-bis-(4,6-di-*t*-butylphenylene)phosphate lithium (NA03) was synthesized and its crystal structural characterization was obtained by single crystal X-ray diffusion. The crystal data showed geometrically the cell parameter of NA03 matched with isotactic polypropylene (iPP), the *a* cell dimension was about two times to the value of cell edge of $(010)_{iPP}$. The disregistry was 2.89%, which was under the upper limit between the lattice matching spacing of host and guest crystals. Then NA03 was proved to be a highly effective nucleating agent for iPP through studying crystallization behaviors, crystallization morphologies, and mechanical properties of iPP nucleated with NA03. The outstanding nucleation efficiency could be attributed to the lattice matching between nucleating agent and iPP. © 2012 Wiley Periodicals, Inc. J Appl Polym Sci 125: 2963–2969, 2012

Key words: poly(propylene); lithium complex; crystal structures; nucleation; lattice matching

INTRODUCTION

Isotactic polypropylene (iPP) is a widely used thermoplastic, combining outstanding mechanical properties and low cost; therefore, its demand is expected to increase. It is a semicrystalline polymer which can crystallize in monoclinic (α), trigonal (β), orthorhombic (γ), and semitic modifications[1–10] with a 3_1 helix conformation but different orientations and packing of the polymer chains in the crystal lattice. Generally, the crystallization rate of semicrystalline polymers like iPP from the melted state depends on two factors: the nucleation rate and spherulites growth rate. Nucleating agent as one of the additives presents a role of increasing the nucleation density of polymer greatly and enhancing the nucleation rate dramatically,[11–16] so it has been widely used in iPP processing to reduce the cycle time and sometimes to improve the optical properties. Although many highly efficient nucleating agents have been developed, the criterion for seeking a new nucleating agent still remains unclear.

Several theories have been proposed to explain how nucleating agent accelerates nucleation rate.[17–21] The most popular one is that "epitaxy" between nucleating agents and crystals controls the nucleation. Epitaxial crystallization was considered the growth of one phase on the surface of a crystal of another phase in one or more strictly defined crystallographic orientation which defined in terms of purely geometric lattice matching.[20,21] Lots of structural studies have shown that epitaxial interaction between polymer and its nucleating agents.[22–28] Shiho Yoshimoto et al. utilized epitaxial crystallization to explain the nucleation effect of a nucleating agent on iPP.[22] As the *c* cell dimension of iPP was very close to the *b* cell dimension of nucleating agent, and further the *a* cell dimension of nucleating agent was about four times the *a* value of iPP cell, the lattice matching existed between two crystal lattices, and then the following epitaxial crystallization took place preferentially: $[010]_{NA}//[001]_{iPP}$ and $(001)_{NA}//(010)_{iPP}$. Mathieu et al. demonstrated that different nucleating agents which acted via different dimensional matching could interact with the same contact face (010) face of iPP.[23] Stocker et al. observed the epitaxial growth of β form iPP on the crystal of a nucleating agent.[24] The results showed that the nucleating agent with about 0.65 nm periodicity and orthogonal geometry of the contact face could induce the β form iPP crystals. Kawai et al. studied the alignment of the iPP crystals

Correspondence to: Z. Xin (xzh@ecust.edu.cn).
Contract grant sponsor: National Natural Science Funds of China; contract grant numbers: 20876042, 20806023.
Contract grant sponsor: The Program of Shanghai Subject Chief Scientist; contract grant number: 10XD1401500.
Contract grant sponsor: Fundamental Research Funds for the Central Universities of China.

induced by *N,N′*-dicyclohexyl-2,6-naphthalenedicarboxamide (DC26NDCA) under a magnetic field.[25] It showed that on the epitaxial surfaces, the *c* axis of the β form iPP modifications aligns parallel to the *b* axis of the nucleating agent and the molecular packing of the β form iPP exhibits a good matching with the surface of the DC26NDCA. In all, the epitaxy crystallization would be occurred when the requirement that crystallographically lattice matching, e.g., a coincidence of unit-cell dimensions, was achieved.

In this work, we considered the lattice matching as the criterion for seeking a new nucleating agent for iPP. A complex, 2,2′-methylene-bis-(4,6-di-*t*-butylphenylene) phosphate lithium (NA03) was synthesized and its crystal structure was obtained by single crystal X-ray diffusion. Geometrically, the *a* cell dimension of NA03 was about two times to the value of cell edge of $(010)_{iPP}$. To evaluate the nucleation efficiency of NA03, crystallization behaviors, crystallization morphologies and mechanical properties of iPP nucleated with NA03 were investigated.

EXPERIMENTAL

Materials

The ligand 2,2′-methylene-bis-(4, 6-di-*t*-butylphenylene) phosphate used in this experimental was provided by Shanghai Kesu Macromolecular Functional Materials, China. The isotactic polypropylene (iPP) (trade name F401, M_w = 307,000, M_n = 81,000, MWD = 3.8) used was kindly provided by Yangzi Petrochemical Corporation (China). The material had a melt flow index (MFI) of 3.4 g/10 min. All the other chemicals were of reagent grade, purchased from commercial sources and used without further purification.

Synthesis

2,2′-Methylene-bis-(4, 6-di-*t*-butylphenylene) phosphate (4.9 g, 10 mmol) was first dissolved in 100 mL methanol, then 50 mL aqueous solution containing $LiOH{\cdot}H_2O$ (0.42 g, 10 mmol) was added dropwise. The mixture was stirred for 2 h under reflux. Precipitation was filtrated and recrystallized in methanol. After slow evaporation, transparent needle-like crystals suitable for single crystal X-ray diffraction study were obtained at room temperature. Yield: 93.5%. EA: Calc for $LiC_{29}H_{42}O_4P$ (CH_3OH): C 68.68%, H 8.76%. Found C 69.77%, H 8.96%. FTIR (KBr): 3425 cm^{-1}(—OH); 2958 cm^{-1}(—CH_3); 1265 cm^{-1}, 1020 cm^{-1} (P—O—Ar); 1097 cm^{-1} (P=O).

Crystal structure

A colorless prismatic crystal of complex having approximate dimensions of 0.43 × 0.38 × 0.37 mm^3 was mounted on a glass fiber. All measurements were collected on a Bruker APEX diffractometer, equipped with CCD area detector and graphite-monochromated Mo Ka radiation. Cell parameters were obtained from 4356 reflections with θ ranging from 4.83° to 52.71°. Cell constants and an orientation matrix for data collection were obtained from a least-squares refinement using the angle θ_{max} = 25.50°. The structure was solved using Fourier techniques. The nonhydrogen atoms were refined anisotropically. Hydrogen atoms were placed in calculated positions (C—H = 0.093–0.098 nm) and were included in the refinement in the riding model approximation, with U_{iso}(H) 1.2–1.5 U_{eq}(C). The C4 and C10 *tert*-butyl groups were rotationally disordered over two orientations with refined site occupancy factors of 0.615 (7) and 0.385 (7). A summary of data collection and structure refinement was given in Table I, selected bond lengths and bond angles were given in Table II and the hydrogen bond within the complex was shown in Table III.

TABLE I
Crystal Data, Data Collection, and Structure Refinement For Complex

Complex	
Empirical formula	$C_{30}H_{46}LiO_5P$
Formula mass	524.58
Crystal system	Monoclinic
Space group	P2(1)/n
a/nm, α/°	1.2722 (16), 90
b/nm, β/°	0.8301 (11), 98.43 (2)°
c/nm, γ/°	3.0244 (4), 90
V/nm^3, *Z*	3.1593 (7), 4
Density(g/cm^{-3}), *F*(000)	1.103, 1136
M(mm)	0.081
θ Range/°	1.66 ~ 25.50
Index range (*h*, *k*, *l*)	−15 ~ 15, −109, −28 ~ 36
Reflections collected	5847
Independent reflections	4283
R_{int}	0.114
Goodness of fit on F^2	1.085
R indices [$I > 2\sigma(I)$]	$R_1 = 0.089$, $wR_1 = 0.208$
R indices (all data)	$R_2 = 0.110$, $wR_2 = 0.220$
Largest difference in peak and hole	0.465~ −0.344

Data collection: Bruker SMART; cell refinement: Bruker SMART; data reduction: Bruker SHELXTL; program(s) used to solve structure: SHELXS97 (Sheldrick, 1990); program(s) used to refine structure: SHELXL97 (Sheldrick, 1997); molecular graphics: Bruker SHELXTL; software used to prepare material for publication: Bruker SHELXTL.[29–32]

Nucleating efficiency

Sample preparation

IPP and NA03 powders were dry-blended by high-speed mixer for 5 min. Then the mixture was extruded by a twin-screw extruder (SJSH-30, Nanjing Rubber and Plastics Machinery Plant) through a

TABLE II
Selected Geometric Parameters: Inter Atomic Distances (nm) and Bond Angles (°) For Complex

	Complex				
P1—O1	0.1465 (2)	P1—O2	0.1492 (2)	P1—O3	0.1610 (2)
P1—O4	0.1610 (3)	P1—Li	0.3059 (6)	Li—O1^{i}	0.1803 (6)
Li—O2	0.1854 (7)	Li—O5	0.1852 (7)	O1—Li^{ii}	0.1803 (6)
O1—P1—O2	120.44 (14)	O1—P1—O3	110.57 (14)	O2—P1—O3	104.61 (13)
O1—P1—O4	109.80 (14)	O2—P1—O4	104.67 (14)	O3—P1—O4	105.67 (13)
O1—P1—Li	93.82 (16)	O2—P1—Li	26.82 (15)	O3—P1—Li	121.49 (17)
O4—P1—Li	114.76 (18)	O1i—Li—O2	120.8 (4)	O1^{i}—Li—O5	117.4 (4)
O2—Li—O5	121.2 (3)	O1^{i}—Li—P1	141.7 (3)	O2—Li—P1	21.30 (12)
O5—Li—P1	99.9 (3)	P1—O1—Li^{ii}	166.8 (3)	P1—O2—Li	131.9 (2)

strand die and pelletized. The pellets were molded into standard test specimens by an injection-molding machine (CJ-80E, Guangdong Zhende Plastics Machinery Plant). The concentration of the nucleating agent was 0.2 wt %. The pure iPP sample was prepared with the same method for comparison.

Crystallization behaviors

DSC (Diamond, Perkin–Elmer) was carried out to study the crystallization behaviors. Temperature was calibrated before the measurements by using Indium as a standard medium. About 3 mg samples were heated from 50 to 200°C at a heating rate of 20°C/min and maintained at 200°C for 5 min to erase thermal history. Then the samples were cooled to 50°C at a cooling rate of 20°C/min. After crystallization, a heating scan at 20°C/min was then run from 50 to 200°C to obtain the final sample enthalpy of fusion.

Crystallization morphologies

The morphology studies of pure iPP and nucleated iPP were performed with the aid of a polarized optical microscopy (BX51, Olympus), attached with a digital camera (DP70), and a hot-stage (THMS600). The samples were placed between two microscopy slides, melted, and pressed at 200°C for 5 min to erase any trace of crystal, and then rapidly cooled to a predetermined crystallization temperature. The samples were kept isothermal until the crystallization process completed, and meanwhile, photographs were automatically taken.

Mechanical properties

The mechanical properties were measured according to ASTM test methods, such as D-638 for the tensile strength and D-790 for the flexural modulus, using a universal testing machine (Shanghai D & G Measure Instrument). The Izod impact strength was tested on the basis of D-256, using an impact tester (Chengde Precision Tester).

TABLE III
Hydrogen Bond For Complex

	Complex			
D—H···A	D—H	H···A	D···A	D—H···A
O5—H5A···O2^{i}	0.0920 (8)	0.1860 (4)	0.2731 (3)	154 (5)

RESULTS AND DISCUSSION

Crystal structure

The structural characterization of the complex was obtained by single crystal X-ray diffusion, which had a monoclinic ($P2(1)/n$) symmetry. Scheme (Scheme 1) and molecular structure (Fig. 1) of the complex were shown below. The Li1 ion was coordinated by two group O atoms (O1^{i} and O2), from the organic ligand and one O atom (O5) from the solvent methanol. Bond lengths and bond angles within the ligand molecule 2, 2′-methylene-bis-(4, 6-di-*t*-butylphenylene) phosphate were close to those reported for the Tris(2,4-di-*tert*-butylphenyl) phosphate.[33] The molecules were linked by Li1—O1^{i} (0.1803 (6) nm), which was shorter than a similar lithium complex with substituted carboxylate ligand.[34] In this way, the polymeric structure along [010] was formed, as shown in Figure 2. Crystal stability was

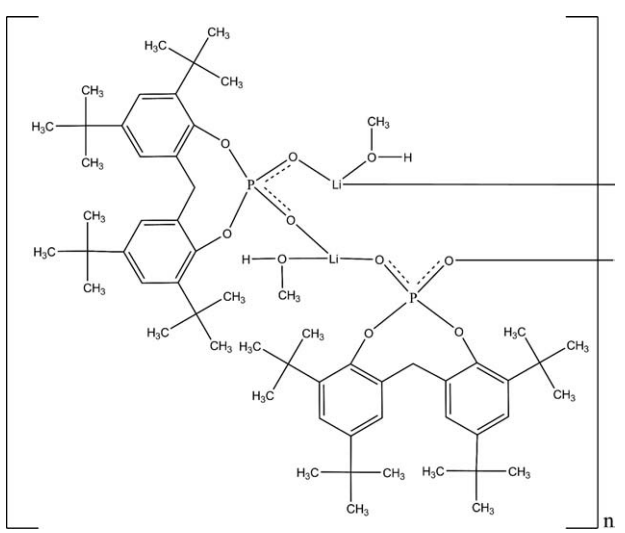

Scheme 1 Structure of the complex.

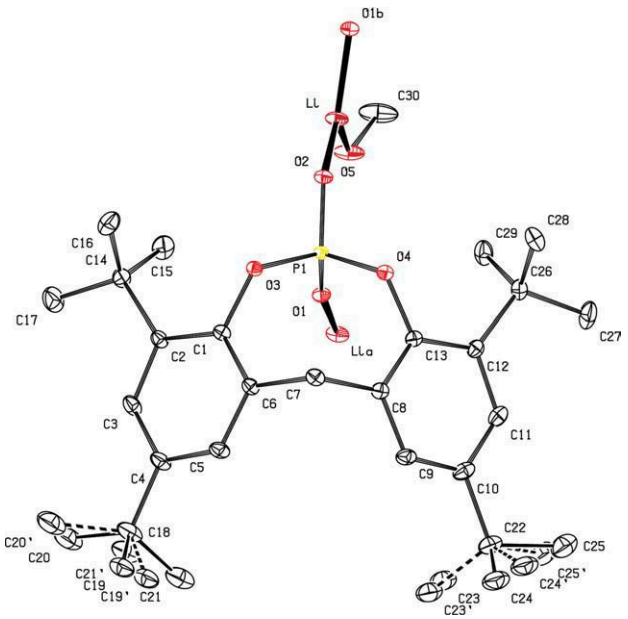

Figure 1 Molecular structure of the complex, with atom labels and 30% probability displacement ellipsoids for non-H atoms. The disordered atoms were shown but the hydrogen atoms were omitted for clarity. [Color figure can be viewed in the online issue, which is available at wileyonlinelibrary.com.]

enhanced by weak intermolecular hydrogen bond O5—H5A···O2^{i}. The geometry was given in Table III. In this hydrogen bond, methanol O5 atoms were donors while O2 atoms from the phosphate acted as acceptors.

The crystal data showed that the complex had a monoclinic unit cell with parameters a = 1.2722 nm, b = 0.8301 nm, and c = 3.0244 nm. It could be noticed that the a cell dimension of NA03 was about two times 0.655 nm, the value of cell edge of $(010)_{iPP}$ (Fig. 3).[23] Wittmann et al. considered epitaxial crystallization was the growth of one phase on the surface of a crystal of another phase in one or more strictly defined crystallographic orientation, and it was often defined in terms of purely geometric lattice matching: 10–15% disregistries between the matching lattice spacing of host and guest crystals were considered as an upper limit.[17,18] The epitaxial relationships determined relied heavily on one or even two dimensional lattice matching. Thus the precondition of this epitaxial behavior was the lattice matching between a crystal and iPP. Mathieu et al. proved the interaction between iPP and three families of nucleating agents with different periodicities matched different cell dimensions of $(010)_{iPP}$.[23] Epitaxy of iPP on benzoic acid rested on the matching of 0.505 nm short diagonal of $(010)_{iPP}$ and 0.516 nm b cell dimension of the acid. 2-bromobenzoic acid crystallized with b parameter of 0.410 nm, which was close to the long diagonal of $(010)_{iPP}$ with the lattice mismatch amounted to 3.66%. The epitaxy on 4-fluorobenzoic acid with b = 0.638 nm matching the value of cell edge of $(010)_{iPP}$ was also described. Crystallographically, lattice matching was found between a cell dimension NA03 and the value of cell edge of $(010)_{iPP}$. The disregistry between the crystal of NA03 and iPP was 2.89%, which was under the upper limit considered by Wittmann et al. Therefore, the epitaxial crystallization could be able to perform

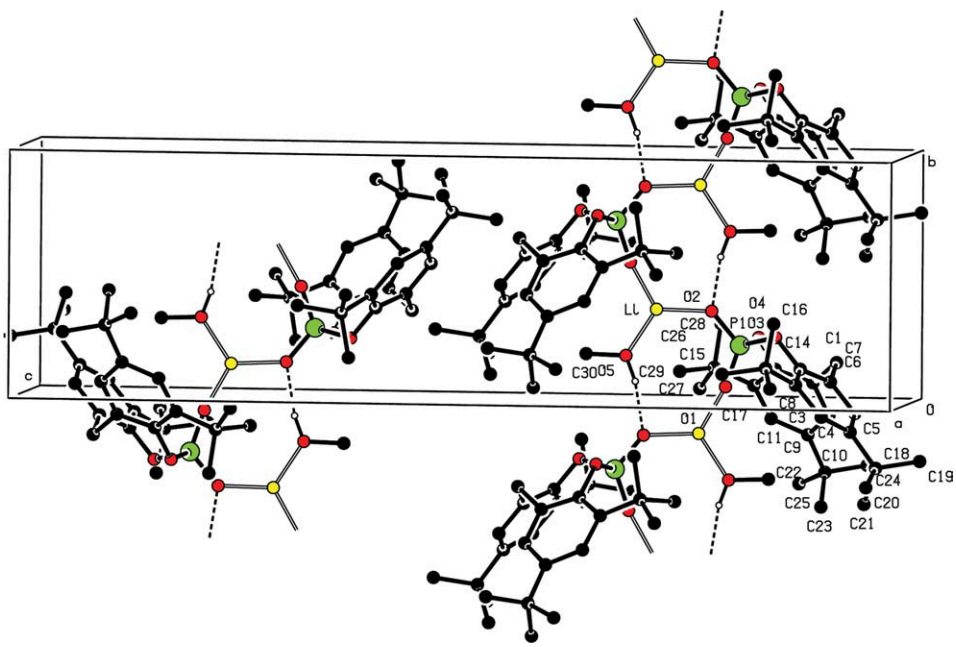

Figure 2 Packing of the complex, viewed down the a axis. H atoms were not involved in hydrogen bonding and disordered atoms had been omitted for clarity. Dash line indicated intermolecular H-bonds. [Color figure can be viewed in the online issue, which is available at wileyonlinelibrary.com.]

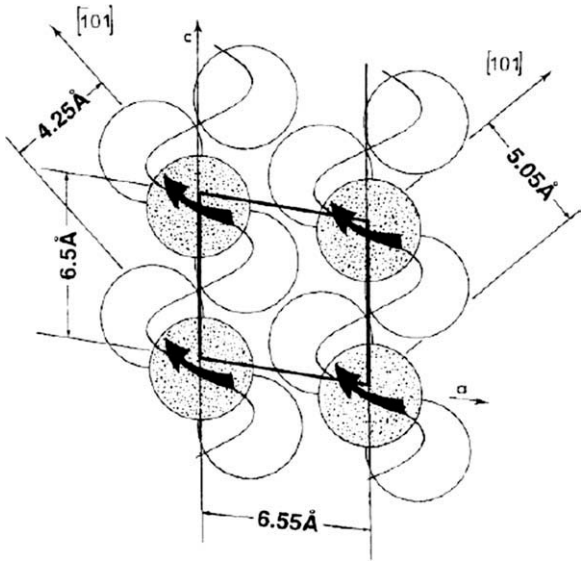

Figure 3 Molecular model of (010) face of α iPP.[23]

between two crystal lattices, indicating that NA03 should have good nucleation ability for iPP. The schematic diagram was shown in Figure 4. To verify it, nucleation efficiency of NA03 on iPP was carried out.

Nucleation efficiency on iPP

Crystallization behaviors

Crystallization behaviors of semicrystalline polymers have a dramatic impact on the mechanical properties, which determines the final applications of polymers. In order to check the effect of the nucleating agent on crystallization behavior, DSC crystallization curves of iPP nucleated with NA03 and pure iPP were plotted in Figure 5. The corresponding crystallization and melting peak temperatures determined from Figure 5 were given in Table IV.

It can be seen from the cooling thermograms that the addition of nucleating agent NA03 could increase the crystallization peak temperature (T_c) of iPP. When 0.2 wt % NA03 was added into iPP, T_c of

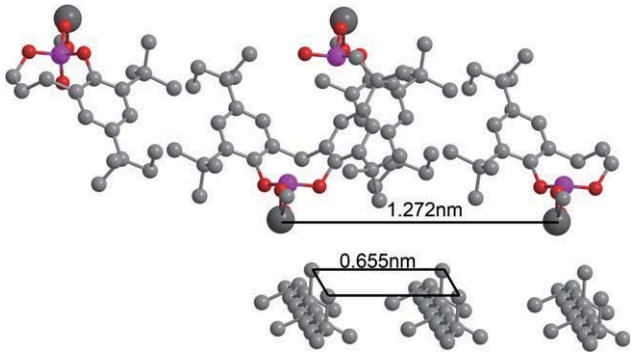

Figure 4 Schematic diagram of cell parameters match between iPP and NA03. [Color figure can be viewed in the online issue, which is available at wileyonlinelibrary.com.]

iPP could be increased from 113.8 to 127.4°C. Moreover, the addition of NA03 made the crystallization peak sharper and scope of crystallization temperature narrower, which indicated that the crystallization rate of nucleated iPP increased significantly.[36] Nucleating agent with crystal lattice matching to iPP may provide extra surfaces onto which the epitaxial growth of iPP lamellae was initiated and then reduced the free energy barrier of nucleation. Therefore, the nucleation of nucleated iPP appeared easier than that of pure iPP, reflecting in the increase of T_c of iPP. As shown in Table IV, melting temperature (T_m) and crystallinity (X_t) of iPP could also be increased when iPP was incorporated with NA03. Because of the increase of T_c, iPP could crystallize at a higher temperature. Thus, the perfection of nucleated iPP increased, which led the melting temperature and crystallinity rising. The T_m of nucleated iPP increased by about 3°C, while the X_t increased by about 5%. Supercooling (ΔT), i.e., the difference between the melting temperature and the crystallization peak temperature, could be a function of the overall rate of crystallization. Beck et al. proposed that the smaller the difference between these temperatures represented the greater the rate of

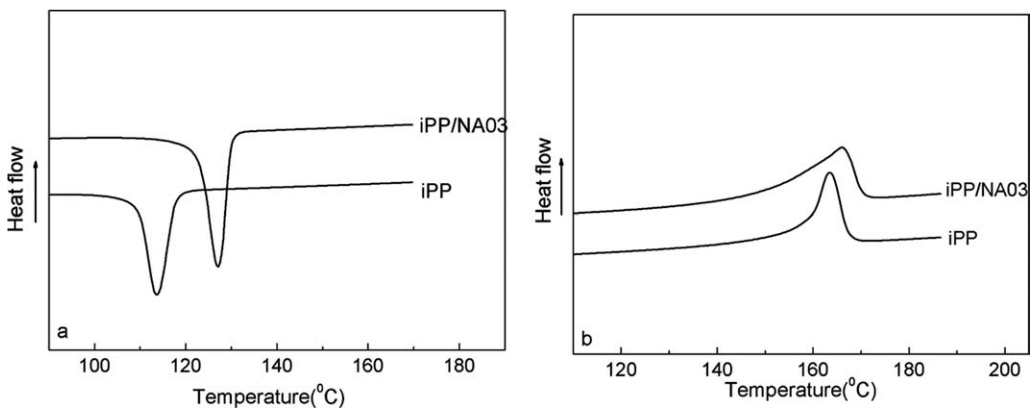

Figure 5 Crystallization and melting curves (a) iPP (b) iPP nucleated with NA03.

TABLE IV
Crystallization and Melting Parameters of iPP and iPP Nucleated with NA03

Index	T_c, °C	T_{onset}, °C	T_{end}, °C	T_m, °C	ΔT*, °C	ΔT_c**, °C	ΔH, J/g	X_t***, %
iPP	113.8	117.8	109.7	163.5	49.7	0	101.4	48.5
iPP/NA03	127.4	130.1	122.9	166.3	38.9	13.6	113.3	54.2

* $\Delta T = T_m - T_c$.
** $\Delta T_c = T_{c_{ipp/NA03}} - T_{c_{ipp}}$.
*** $X_t = \Delta H/\Delta H_f \times 100\%$[35] (here, H_f is 209 J/g for iPP).

crystallization.[37] From the table, ΔT of iPP nucleated with NA03 decreased by 10.8°C which suggested that the rate of iPP crystallization was developed with the presence of NA03. ΔT_c was the difference in crystallization peak temperature between pure iPP and nucleated iPP. Rybnikar rated the nucleating efficiency of nucleating agents by investigating ΔT_c of them.[38] The classification of nucleating efficiency was: $\Delta T_c \geq 6.5$°C, high; $\Delta T_c = 5$–6.5°C medium; $\Delta T_c = 3$–5°C low. Obviously, NA03 could be considered as a highly efficiency nucleating agent for iPP.

Crystallization morphologies

We employed polarized optical microscope (POM) to observe the crystallization morphologies. Polarized optical micrographs of virgin iPP and nucleated iPP crystallized under isothermal conditions (140°C) were shown in Figure 6.

As seen in Figure 6, the addition of NA03 could decrease the spherulite size of iPP remarkably. Figure 6(a) showed that owing to the low nucleation rate and lack of nuclei in pure iPP, the spherulite grew into a large size one before it impinged another spherulite. Crystallization could be divided into two parts: nucleation and crystal growth. The formation of nuclei was difficult in pure iPP, thus spherulite developed mainly in a homogeneous nucleation way, followed by nucleation-controlled spherulite growth. While in nucleated iPP, a large number of nuclei would be produced because of the existence of nucleating agents. Because of the epitaxial crystallization, the nucleation rate of nucleated iPP would be very high. Then the crystallization would be in a heterogeneous nucleation way, followed by a diffusion-controlled spherulite growth. Hence, the spherulite cannot grow large enough to overlap, resulting that the size of spherulites in nucleated iPP would be much smaller than those in pure iPP [Fig. 6(b)].

Mechanical properties

From the view point of industrial application, it is necessary to investigate the effects of nucleating agent on mechanical properties. The effects of the nucleating agent NA03 on mechanical properties of iPP were given in Table V.

Table V showed that the addition NA03 could obviously improve the mechanical and optical properties of iPP. Mechanical and optical properties of iPP would be enhanced because of the increase in the crystallinity and decrease in the spherulite size of iPP.[39] With 0.2 wt % NA03, the tensile strength of iPP increased by 10.35%, flexural modulus improved by 33.54% while haze value of iPP decreased by 45.26%.

All these studies showed that NA03 was a highly effective nucleating agent for iPP. The outstanding efficiency could be attributed to the lattice matching between nucleating agent and iPP. Nucleation densities were higher when lattice matching was approached, so that iPP crystallized at higher temperature and the spherulite size of iPP decreased significantly. Further, the mechanical and optical properties of iPP improved.

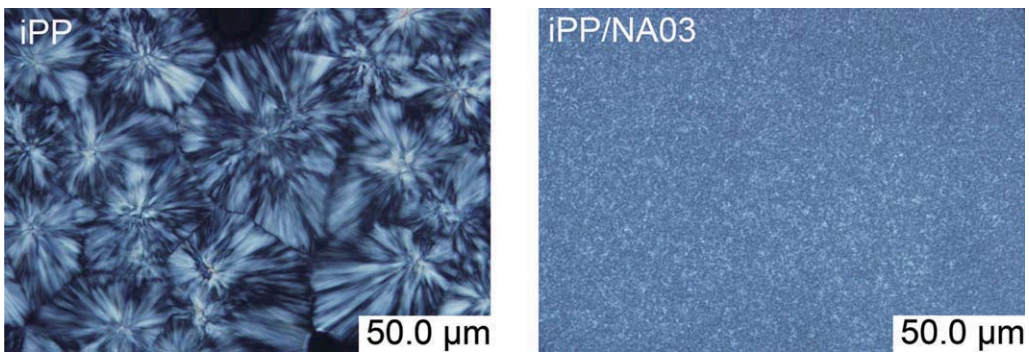

Figure 6 Polarized light microphotographs (a) iPP (b) iPP nucleated with NA03 crystallized at 140°C. [Color figure can be viewed in the online issue, which is available at wileyonlinelibrary.com.]

TABLE V
Mechanical Properties of iPP and iPP Nucleated with NA03

Index	Tensile strength (MPa)	Tensile modulus (MPa)	Flexural strength (MPa)	Flexural modulus (MPa)	Impact strength (J/m)	Haze value (%)
iPP	33.73	983	43.79	1261	35.27	83.55
iPP/NA-03	37.22	1101	54.68	1684	32.94	45.9

CONCLUSIONS

In this work, a complex, 2,2′-methylene-bis-(4, 6-di-*t*-butylphenylene) phosphate lithium (NA03) was synthesized. The crystal structural characterization of NA03 was investigated by single crystal X-ray diffusion. The results showed that the molecules were bonded by Li1—$O1^{i}$, forming a polymeric chain along [010], and the crystal structure was further stabilized by O5-H5A···$O2^{i}$ intermolecular hydrogen bonding. From the point view of geometric, the *a* cell dimension of NA03 was about two times to the value of cell edge of $(010)_{iPP}$. The disregistry, with the value of 2.89%, was under the upper limit between the matching lattice spacing of host and guest crystals, indicating the lattice matching could be able to be performed between two crystal lattices. Then, the crystallization behaviors, crystallization morphologies and mechanical properties of iPP and iPP nucleated with NA03 were investigated. When 0.2 wt % NA03 was added into iPP, crystallization peak temperature of iPP can be increased from 113.8 to 127.4°C and the spherulite size of iPP remarkably decreased. Meanwhile the tensile strength of iPP was increased by 10.35%, flexural modulus of iPP was able to be enhanced by 33.54%, and haze value of iPP could be decreased by 45.26%. All these studies showed that NA03 was a highly effective nucleating agent for iPP. The outstanding nucleation efficiency may due to the lattice matching between nucleating agent and iPP. A compound can serve as a nucleating agent when it meets the requirement that crystallographically lattice matching, e.g., a coincidence of unit-cell dimensions.

References

1. Vagar, J. J Mater Sci 1992, 27, 2557.
2. Naiki, M.; Kikkawa, T.; Endo, Y. Nozaki, K.; Yamamoto, T.; Hara, T. Polymer 2000, 42, 5471.
3. Lotz, B.; Wittmann, J. C.; Lovinger, A. J. Polymer 1996, 37, 4979.
4. Awaya, H. Polymer 1998, 29, 591.
5. Dorset, D. L.; McCourt, M. P.; Kopp, S.; Schumacher, M.; Okihara, T.; Lotz, B. Polymer 1998, 39, 6331.
6. Busse, K.; Kressler, J.; Maier, R. D.; Scherble, J. Macromolecules 2003, 33, 8775.
7. Norton, D. R.; Keller, A. Polymer 1985, 26, 704.
8. Lotz, B.; Wittmann, J. C. J Polym Sci Part B Polym Phys 1986, 24, 1541.
9. Wang, Z. G.; Phillips, R. A.; Hsiao, B. S. J Polym Sci Part B: Polym Phys 2000, 38, 2580.
10. Bruckner, S.; Meille, S. V.; Petraccone, V.; Pirozzi, B. Prog Polym Sci 1991, 16, 361.
11. Romankiewicz, A.; Tomasz, S.; Brostow, W. Polym Int 2004, 53, 2086.
12. Tenma, M.; Yamaguchi, M. Polym Eng Sci 2007, 47, 1141.
13. Kristiansen, M.; Werner, M.; Tervoort, T.; Smith, P.; Blomenhofer, M.; Schmidt, H. W. Macromolecules 2003, 36, 5150.
14. Gui, Q.; Xin, Z.; Zhu, W. P.; Dai, G. C. J Appl Polym Sci 2003, 88, 297.
15. Li, C.; Isshiki, N.; Saito, H.; Ogata, K.; Toyota, A. J Polym Sci Part B Polym Phys 2009, 47, 130.
16. Li, C.; Isshiki, N.; Saito, H.; Kohno, K.; Toyota, A. J Appl Polym Sci 2010, 115, 1098.
17. Binsbergn, F. L. Polymer 1970, 11, 253.
18. Binsbergn, F. L. Polymer 1970, 11, 309.
19. Binsbergn, F.L. J Polym Sci Part B: Polym Phys 1973, 11, 117.
20. Wittmann, J. C.; Lotz, B. J Polym Sci Part B Polym Phys 1981, 19, 1837.
21. Wittmann, J. C.; Lotz, B. Prog Polym Sci 1990, 15, 909.
22. Yoshimoto, S.; Ueda, T.; Yamanaka, K.; Kawaguchi, A.; Tobita, E.; Haruna, T. Polymer 2001, 42, 9627.
23. Mathieu, C.; Thierry, A.; Lotz, B.; Wittmann, J. C. Polymer 2000, 41, 7241.
24. Stocker, W.; Schumacher, M.; Graff, S. Macromolecules 1998, 31, 807.
25. Kawai, T.; Iijima, R.; Yamamoto, Y.; Kimura, T. Polymer 2002, 43, 7301.
26. Haubruge, H. G.; Daussin, R.; Jonas, A. M.; Legras, R.; Wittmann, J. C.; Lotz, B. Macromolecules 2003, 36, 4452.
27. Yan, S.; Petermann, J. J Polym Sci Part B Polym Phys 2000, 38, 80.
28. Sun, Y.; Li, H.; Huang, Y.; Chen, E.; Gan, Z.; Yan, S. Polymer 2006, 47, 2455.
29. Bruker. SMART and SAINT. 1998, Bruker AXS Inc., Madison, Wisconsin, USA.
30. Sheldrick, G. M. Acta Cryst A 1990, 46, 467.
31. Sheldrick, G. M. SHELXTL. Version 5.10. 1997b, Bruker AXS Inc., Madison, Wisconsin, USA.
32. Sheldrick, G. M. SADABS. 1996, University of Göttingen, Germany.
33. Vinuchakkaravarthy, T.; Sangeetha, C. K.; Velmurugan, D. Acta Cryst 2010, E66, o2207.
34. Fun, H. K.; Balasubramani, K.; Rai, S.; Shetty, P.; Isloord, A. M. Acta Cryst 2010, E65, m917.
35. Phillips, R.; Manson J. A. E. J Polym Sci Polym Phys 1997, 35, 875.
36. Chen, Y.; Xu, M. Acta Polymerica Sinica 1998, 6, 671.
37. Beck, H. N.; Ledletter, H. D. J Appl Polym Sci 1965, 9, 2131.
38. Rybnikar, F. J Appl Polym Sci 1969, 13, 827.
39. Pukanszky, B.; Mudra, I.; Staniek, P. J Vinyl Additive Tech 1997, 3, 53.